Xu et al. Nanoscale Research Letters (2018) 13:292
https://doi.org/10.1186/s11671-018-2706-z

Nanoscale Research Letters

NANO EXPRESS Open Access

# Enhanced Visible Light-Responsive Photocatalytic Properties of Ag/$BiPbO_2Cl$ Nanosheet Composites

Ai Jiao Xu, Shang Shen Feng*, Shi Jie Shen, Yan Ping Liu and Wen Wu Zhong*

## Abstract

Ag/$BiPbO_2Cl$ nanosheet composites were successfully prepared by hydrothermal synthesis and photo-reduction. The morphology, microstructure, and optical properties of the as-prepared Ag/$BiPbO_2Cl$ nanosheet composites were characterized using TEM, XRD, and UV-Vis diffuse reflection spectroscopy. The prepared Ag/$BiPbO_2Cl$ nanosheet composites with 0.5 wt% Ag exhibit favorable photocatalytic activity, which is 3.6 times that of $BiPbO_2Cl$ nanosheet. The enhanced photocatalytic properties can be attributed to the inner electromagnetic field, higher visible light response range, excellent conductivity, and lower Fermi level of Ag.

**Keywords:** Photocatalysis, Co-catalyst, Hydrothermal, Bismuth-based semiconductor

## Background

In recent years, environmental pollution has become increasingly serious. In order to solve the problem of organic pollutants, semiconductor photocatalytic materials have been widely adopted due to their unique advantages [1–4]. ZnO, $TiO_2$, and other wide bandgap semiconductors are popular in photocatalytic degradation of organic pollutants [5–8]. However, wide bandgap semiconductors can only absorb ultraviolet lights, which limits the application prospects of these catalysts. Therefore, it is necessary to search for photocatalytic materials that are responsive to visible lights [9, 10].

Bismuth-based semiconductor photocatalysts possess rich structural characteristics and suitable valence band positions, which can satisfy the requirements of organic matter decomposition [11, 12]. Among them, $BiPbO_2Cl$ is considered to be commendable due to its narrow band gap, built-in electric field between [$BiPbO_2$] and [Cl] plates, and hybrid band structure [13, 14]. Nevertheless, the fast electron-hole recombination rate limits its application in the field of photocatalysis.

It has been reported that the combination of semiconductor photocatalytic materials with noble metals or graphene can improve their photocatalytic properties [15, 16]. This is because the recombination rate of photo-generated electrons and holes decreases after compounding. Noble metals, such as Au, Ag, and Pt, have been used as electron acceptors to separate the photo-generated electron and holes [17, 18].

In this paper, the Ag/$BiPbO_2Cl$ composite photocatalyst was synthesized by hydrothermal method and photo-reduction for improving the photocatalytic properties of $BiPbO_2Cl$ nanosheets. The prepared Ag/$BiPbO_2Cl$ nanosheet composites with 0.5 wt% Ag exhibit favorable photocatalytic activity, which is 3.6 times that of $BiPbO_2Cl$ nanosheet.

## Methods

### Preparation of Ag/$BiPbO_2Cl$ Nanosheet Composites

The $BiPbO_2Cl$ nanosheets were prepared through one-step hydrothermal method as we used before [13]. The Ag/$BiPbO_2Cl$ composites were synthesized by photo-reduction. The obtained $BiPbO_2Cl$ (1 mmol) was dispersed in 20 mL deionized water with the aid of magnetic stirring, and then, an appropriate amount of $AgNO_3$ was added. The suspension was then irradiated with a 500-W Xe lamp with stirring at room temperature for 3 h, with light being cut off below 420 nm using a cut-off filter. The resulting granules were washed with deionized water to remove residual organic matter and dried in air at 80 °C for 2 h. In order to study the effect of Ag content on the photocatalytic activity

* Correspondence: fss@tzc.edu.cn; tianmenwenwu@163.com
Department of Materials, Taizhou University, Taizhou 318000, China

of $BiPbO_2Cl$, the added contents of Ag were denoted as 0.25, 0.5, and 0.75 wt%.

### Photocatalytic Activities

The photocatalytic activity was characterized in a XPA series photochemical reaction instrument by a 500-W Xe lamp with a cutoff filter of 420 nm. The characterization of photocatalytic activity of samples was used by methyl orange (MO) as organic dyes. During the photocatalytic performance test, 50 mg $Ag/BiPbO_2Cl$ nanosheet composite powders was added into 50 mL MO aqueous solution (10 mg/L) with continuous stirring for 1 h in the dark. The absorption spectra of the solution were collected on a Shimadzu UV-2700 spectrometer.

### Sample Characterization

The powder's X-ray diffraction (XRD) patterns were measured on a PANalytical X'Pert Pro X-ray diffractometer with Cu Kα radiation (1.54178 Å). The surface morphology was obtained on the scanning electron microscope (SEM, Hitachi S-4800). Transmission electron microscope (TEM) morphology was measured on a JEOL JEM-2011 TEM. The UV-vis diffuse reflectance spectra were measured on Shimadzu UV-2450. The X-ray photoelectron spectroscopy (XPS) was measured on a Pekin Elmer PHI-5300 XPS. The photoluminescence (PL) emission spectra were measured on a Shimadzu RF-5301 with excitation wavelength at 320 nm.

## Results and Discussion

Photocatalytic activity of the $BiPbO_2Cl$ and $Ag/BiPbO_2Cl$ composites has been evaluated with degradation of MO under illumination of visible light (> 420 nm). The concentration of the MO liquid is characterized by the relative absorption strength at 464 nm. Figure 1a shows the visible light photocatalytic activity of the $BiPbO_2Cl$ and $Ag/BiPbO_2Cl$ composites. Prior to degradation, the MO solution containing the photocatalyst was stirred for 1 h in the dark environment to achieve adsorption equilibrium. From Fig. 1a, it can be concluded that the photocatalytic efficiency of the $BiPbO_2Cl$ composites increases with the increase of Ag content, reaching a maximum when the Ag content is 0.5 wt%. This may be due to the absorption of photo-generated electrons by Ag, resulting in a decrease in the photo-generated electron-hole recombination rate, thereby increasing its photocatalytic activity. As the Ag content further increases, its photocatalytic efficiency decreases. When the content of Ag further increases, the content of $BiPbO_2Cl$ correspondingly decreases, resulting in a decrease in the number of photo-generated carriers and so as the photocatalytic activity. Figure 1b shows the photocatalytic reaction kinetics of the $BiPbO_2Cl$ and $Ag/BiPbO_2Cl$ composites. From Fig. 1b, we can draw that the MO degradation rate over $Ag/BiPbO_2Cl$ composites (0.0158 $min^{-1}$) is about 3.6 times that of the $BiPbO_2Cl$ (0.0044 $min^{-1}$).

In order to study the morphology and microstructure, SEM, TEM, and XRD were adopted for studying the $BiPbO_2Cl$ and $Ag/BiPbO_2Cl$ composites. From Fig. 2a, one can see that $BiPbO_2Cl$ is featured as nanosheets, with thickness of about 12 nm. Figure 2b shows the SEM morphology of 0.5 wt% $Ag/BiPbO_2Cl$ composites; the silver nanoparticles are randomly distributed on the surface of the nanosheet $BiPbO_2Cl$. The diameter of Ag particles is about 10 nm. The HRTEM (Fig. 2c) images also reveal the existence of Ag. The existence of Ag is further evidenced by XPS. Figure 2d shows the XRD of $BiPbO_2Cl$ and 0.5 wt% $Ag/BiPbO_2Cl$ composites. Compared with the XRD pattern of the $BiPbO_2Cl$, the pattern of $Ag/BiPbO_2Cl$ composites has no obvious changes, which may result from the low amount of Ag. The compositional analysis is measured by EDS (Fig. 3). Bi, Pb, O, Cl, and Ag

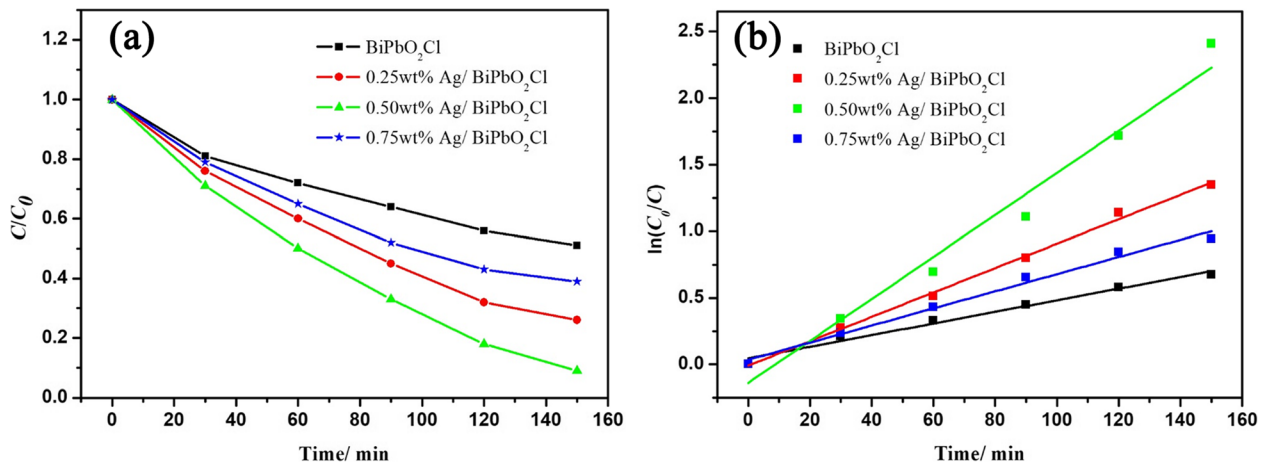


**Fig. 1** **a** Photocatalytic degradation of MO with $BiPbO_2Cl$ and $Ag/BiPbO_2Cl$ composites. **b** Kinetics of MO decolorization in solutions

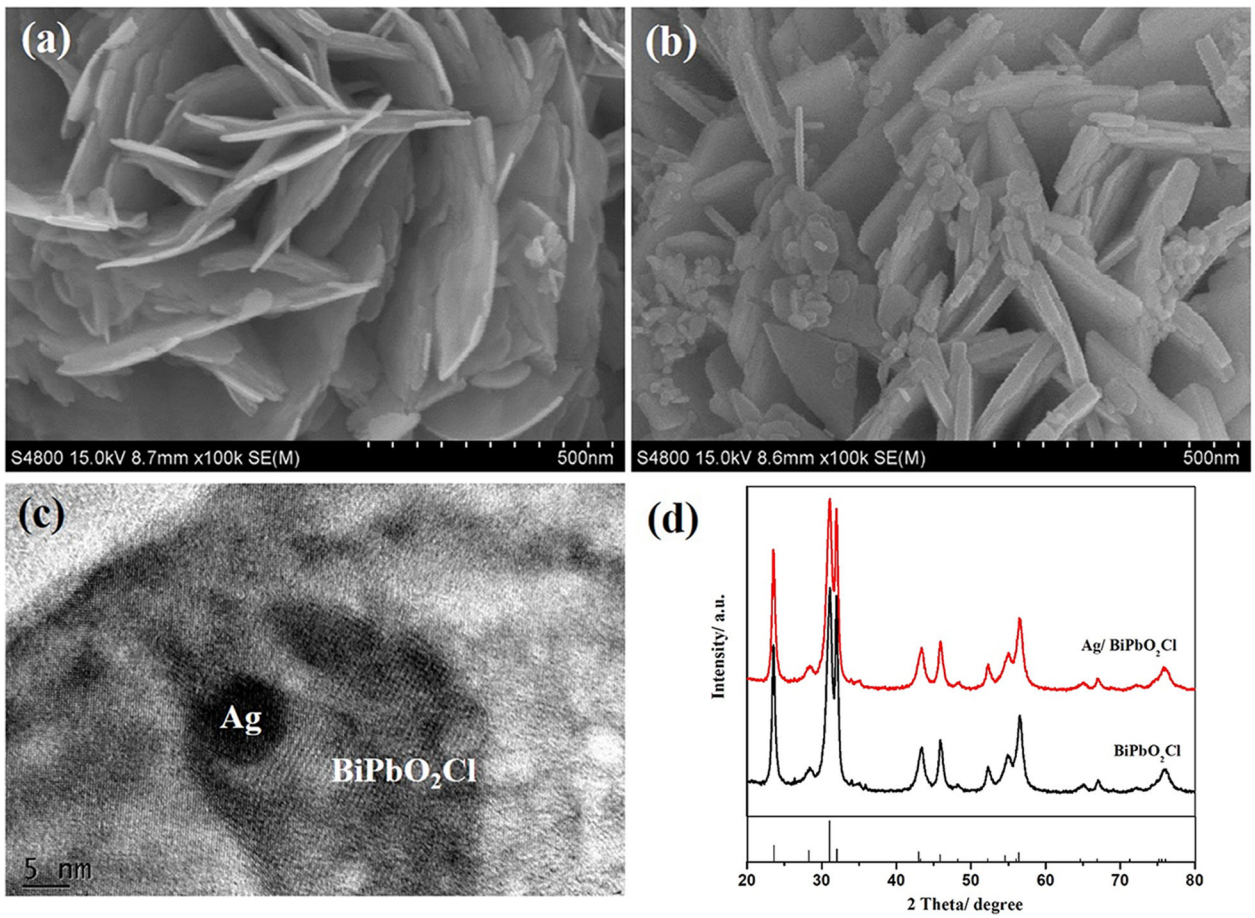


**Fig. 2** The SEM of $BiPbO_2Cl$ (**a**) and 0.5 wt% Ag/$BiPbO_2Cl$ composites (**b**). **c** High-resolution TEM image of the 0.5 wt% Ag/$BiPbO_2Cl$ composites. **d** XRD of samples

elements are observed in the sample. Moreover, the EDS elemental mappings indicate that Ag element is evenly distributed throughout Ag/$BiPbO_2Cl$ composites.

In order to study the surface chemical state of the sample, the XPS analysis was adopted for studying the Ag/$BiPbO_2Cl$ composites. As shown in Fig. 4a, the presence of Bi, Pb, O, Cl, and Ag could be observed in the XPS spectrum. As shown in Fig. 4b, the peaks of Bi $4f_{7/2}$ and Bi $4f_{5/2}$ are located at 159.1 and 164.5 eV, respectively, which are consistent with the characteristic of $Bi^{3+}$ [19, 20]. The peaks of Pb $4f_{7/2}$ and Pb $4f_{5/2}$ are located at 137.9 and 142.8 eV (Fig. 4c), which are consistent with the characteristic of $Pb^{2+}$ [21]. The peak of O 1s is located at 529.8 eV, which belongs to $O^{2-}$ from the Bi–O bond (Fig. 4d). As displayed in Fig. 4e, two peaks of Cl 2p are at 197.8 and 199.4 eV, which are consistent with the characteristic of $Cl^{1-}$ [22]. As shown in Fig. 4f, two peaks of 368.1 and 374.3 eV are observed, which correspond to Ag $3d_{3/2}$ and Ag $3d_{5/2}$, respectively. According to the results reported by Zhang et al. [23], the peaks at 368.6 and 374.6 eV can be attributed to $Ag^0$.

Compared with the yellow $BiPbO_2Cl$ nanosheets, the color of the Ag/$BiPbO_2Cl$ composites becomes darker with the increase of Ag content. The UV-vis absorption spectra of $BiPbO_2Cl$ and Ag/$BiPbO_2Cl$ composites are shown in Fig. 5a. The strong absorption below a wavelength of 600 nm is associated with the optical band gap of $BiPbO_2Cl$. After loading Ag on the surface of $BiPbO_2Cl$, the absorbance at the range of 450–800 nm is higher than that of pure $BiPbO_2Cl$, which is due to the absorption characteristic of surface plasmon caused by the composite of Ag and $BiPbO_2Cl$ [24]. As a result, after the loading of Ag on the surface of $BiPbO_2Cl$, the visible light response range of $BiPbO_2Cl$ is increased. The band gap calculated from Fig. 5a is shown in Fig. 5b. After compounding with Ag, the band gap of $BiPbO_2Cl$ decreases from 2.05 to 1.68 eV. In addition, the photoluminescence emission spectra of $BiPbO_2Cl$ and Ag/$BiPbO_2Cl$ composites are carried out to reflect the recombination rate of photo-generated electrons and holes. As shown in Fig. 5c, the PL intensity is decreased drastically after the loading of Ag on the surface of

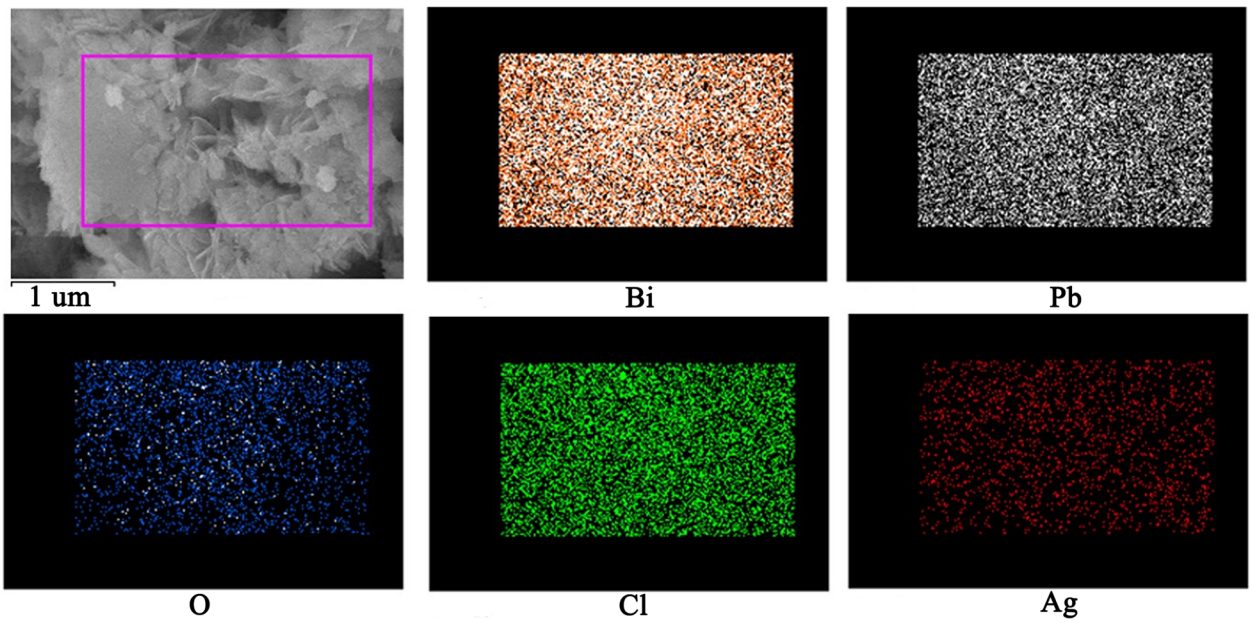


**Fig. 3** EDS mapping of element of Ag/$BiPbO_2Cl$ composites

$BiPbO_2Cl$, which is attributed to the fast transfer of photo-generated electrons from $BiPbO_2Cl$ to Ag, leading to reduction of recombination rate of photo-generated electrons and holes [25].

The principle of high photocatalytic activity for Ag/$BiPbO_2Cl$ composites is as follows. First of all, the visible light response range is increased by the composition of Ag and $BiPbO_2Cl$. Secondly, the loading of Ag on the surface of $BiPbO_2Cl$ could generate the inner electromagnetic field. When the $BiPbO_2Cl$ semiconductor surface is in contact with Ag, redistribution of carriers is realized. Since the Fermi level of Ag is lower than that of $BiPbO_2Cl$ [26], the photo-excited electrons transfer from the $BiPbO_2Cl$ to Ag particles until their Fermi level is the same, thus forming the built-in field, as shown in Fig. 6b. The photo-generated electron will transfer quickly from $BiPbO_2Cl$ to Ag with the help of the inner electromagnetic field and excellent conductivity of Ag. Thirdly, as shown in Fig. 6a, the electrons generated by $BiPbO_2Cl$ will reduce the molecular $O_2$ to form the $O_2\bullet$ active species [27]. On the other side, the photo-generated holes tend to remain on the surface of $BiPbO_2Cl$. And then, these holes will

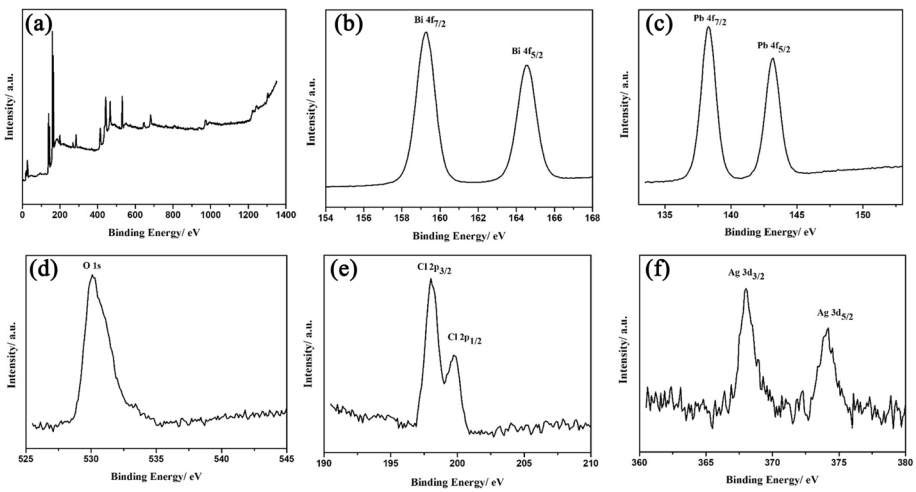


**Fig. 4** The XPS spectra of Ag/$BiPbO_2Cl$ composites. **a** Survey, **b** Bi 4f, **c** Pb 4f, **d** O 1s, **e** Cl 2p, and **f** Ag 3d

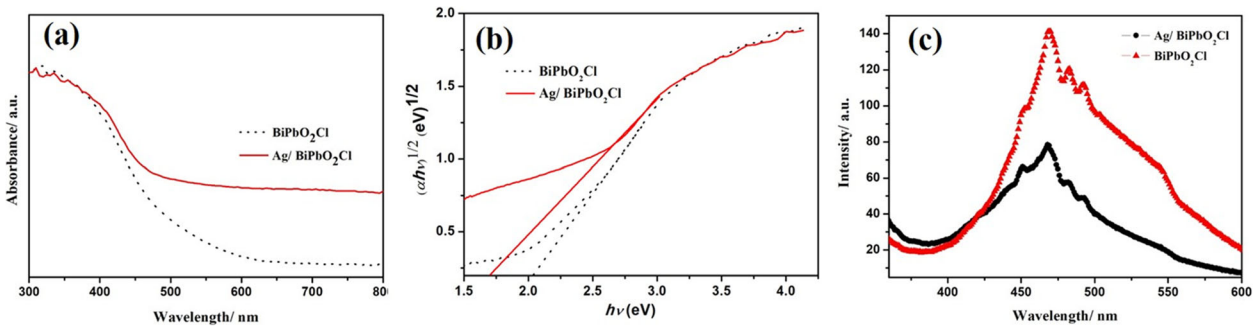


**Fig. 5** The UV-vis absorption spectra (**a**) and photoluminescence emission spectra (**b**) of $BiPbO_2Cl$ and 0.5 wt% Ag/$BiPbO_2Cl$ composites (**c**)

transform the water molecules on the surface of $BiPbO_2Cl$ into OH• active species. Under the effect of these active species of $O_2$• and OH•, the MO molecules are decomposed into $CO_2$ and $H_2O$. These results indicate that the loading of Ag on the surface of $BiPbO_2Cl$ could produce high visible light photocatalytic activity.

## Conclusions

In summary, highly efficient Ag/$BiPbO_2Cl$ composites were prepared by hydrothermal synthesis and photo-reduction. The obtained 0.5 wt% Ag/$BiPbO_2Cl$ nanosheet composite material has better photocatalytic activity, which is 3.6 times that of $BiPbO_2Cl$ nanosheets. After $BiPbO_2Cl$ nanosheets and Ag are composited, the visible light response range increases and the electron-hole recombination rate decreases, thus improving the visible light photocatalytic properties. The excellent photocatalytic property of Ag/$BiPbO_2Cl$ composites are attributed to the inner electromagnetic field, higher visible light response range, excellent conductivity, and lower Fermi level of Ag.

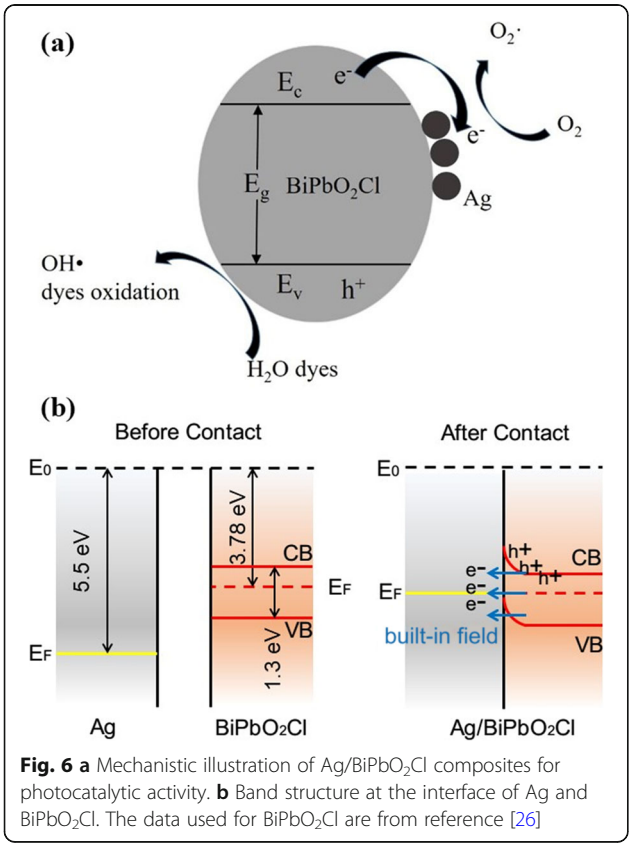


**Fig. 6 a** Mechanistic illustration of Ag/$BiPbO_2Cl$ composites for photocatalytic activity. **b** Band structure at the interface of Ag and $BiPbO_2Cl$. The data used for $BiPbO_2Cl$ are from reference [26]

### Abbreviations

DRS: Diffuse reflection spectroscopy; MO: Methyl orange; TEM: Transmission electron microscope; XRD: X-ray diffraction

### Acknowledgements

We acknowledge financial support from the National Natural Science Foundation of China (Grant No. 51572183) and the Natural Science Foundation of Zhejiang Province, China (Grant No. LY15E010002).

### Availability of Data and Materials

The datasets generated during and/or analyzed during the current study are available from the corresponding author on request.

### Authors' Contributions

SF and WZ designed this work. AX and SS performed the experiments. AX and YL analyzed the data. AX and WZ wrote this paper. All authors read and approved the final manuscript.

### Competing Interests

The authors declare that they have no competing interests.

## Publisher's Note



Received: 19 July 2018 Accepted: 3 September 2018
Published online: 21 September 2018

### References

1. He RA, Cao SW, Zhou P, Yu JG (2014) Recent advances in visible light Bi-based photocatalysts. Chin J Catal 35:989–1007
2. LiangYC CCC, Lin TY, Cheng YR (2016) Synthesis and microstructure-dependent photoactivated properties of three-dimensional cadmium sulfide crystals. J Alloy Compd 688 Part A:769–775
3. Zhong WW, Lou YF, Jin SF, Wang WJ, Guo LW (2016) A new Bi-based visible-light-sensitive photocatalyst $BiLa_{1.4}Ca_{0.6}O_{4.2}$: crystal structure, optical property and photocatalytic activity. Sci Rep 6(23235):1–6
4. Fu JW, Yu JG, Jiang CJ, Cheng B (2018) g-$C_3N_4$-based heterostructured photocatalysts. Adv Energy Mater 8:1701503
5. Fang ZB, Wang YY, Xu DY, Tan YS, Liu XQ (2004) Blue luminescent center in ZnO films deposited on silicon substrates. Optical Mater 26:239–242

6. Hoffmann MR, Martin ST, Choi W, Bahnemann DW (1995) Environmental applications of semiconductor photocatalysis. Chem Rev 95:69–96
7. Fujishima R, Morikawa T, Okwaki T, Aoki K, Taga Y (2001) Visible-light photocatalysis in nitrogen-doped titanium oxides. Science 293:269–271
8. Chen XB, Burda C (2008) The electronic origin of the visible-light absorption properties of C-, N- and S-doped $TiO_2$ nanomaterials. J Am Chem Soc 130: 5018–5019
9. Amano F, Yamakata A, Nogami K, Osawa M, Ohtani B (2008) Visible light responsive pristine metal oxide photocatalyst: enhancement of activity by crystallization under hydrothermal treatment. JAm Chem Soc 130:17650–17651
10. Wang DF, Kako T, Ye JH (2008) Efficient photocatalytic decomposition of acetaldehyde over a solid-solution perovskite $(Ag_{0.75}Sr_{0.25})(Nb_{0.75}Ti_{0.25})O_3$ under visible-light irradiation. J Am Chem Soc 130:2724–2725
11. Chen XL, Liang JK, Liu Y, Lan YC, Zhang YM, Che GC, Liu GD, Xing XY, Qiao XY (1999) Structural transformations of $Bi_2CuO_4$ induced by mechanical deformation. J Appl Phys 85:3155–3158
12. Chen XL, Eysel W, Li JQ (1996) $Bi_2La_4O_9$: a monoclinic phase in the system $Bi_2O_3$–$La_2O_3$. J Solid State Chem 124:300–304
13. Zhong WW, Li DD, Jin SF, Wang WJ, Yang XA (2015) Synthesis and structure of $BiPbO_2Cl$ nanosheet with enhanced visible light photocatalytic activity. Appl Surf Sci 356:1341–1344
14. Shan ZS, Lin XP, Liu ML, Ding HM, Huang FQ (2009) A Bi-based oxychloride $PbBiO_2Cl$ as a novel efficient photocatalyst. Solid State Sci 11:1163–1169
15. Chowdhury S, Balasubramanian R (2014) Graphene/semiconductor nanocomposites (GSNs) for heterogeneous photocatalytic decolorization of wastewaters contaminated with synthetic dyes: a review. Appl Catal B Environ 160-161:307–324
16. Xu C, Xu YL, Zhu JL (2014) Photocatalytic antifouling graphene oxide-mediated hierarchical filtration membranes with potential applications on water purification. ACS Appl Mater Interfaces 6:16117–16123
17. Lin F, Wang DG, Jiang ZX, Ma Y, Li J, Li RG, Li C (2012) Photocatalytic oxidation of thiophene on $BiVO_4$ with dual co-catalysts Pt and $RuO_2$ under visible light irradiation using molecular oxygen as oxidant. Energy Environ Sci 5:6400–6406
18. Lin HX, Ding LY, Pei ZX, Zhou YG, Long JJ, Deng WH, Wang XX (2014) Au deposited BiOCl with different facets: on determination of the facet-induced transfer preference of charge carriers and the different plasmonic activity. Appl Catal B Environ 160-161:98–105
19. Ye L, Deng K, Xu F, Tian L, Peng T, Zan L (2012) Increasing visible-light absorption for photocatalysis with black BiOCl. Phys Chem Chem Phys 14:82–85
20. Hu JL, Fan WJ, Ye WQ, Huang CJ, Qiu XQ (2014) Insights into the photosensitivity activity of BiOCl under visible light irradiation. Appl Catal B Environ 158-159:182–189
21. Babuka T, Kityk IV, Parasyuk OV, Myronchuk G, Khyzhun OY, Fedorchuk AO, Makowska-Janusik M (2015) Origin of electronic properties of $PbGa_2Se_4$ crystal: experimental and theoretical investigations. J Alloy Comd 633:415–423
22. Wang C, Shao C, Liu Y, Zhang L (2008) Photocatalytic properties BiOCl and $Bi_2O_3$ nanofibers prepared by electrospinning. Scr Mater 59:332–335
23. Zhang H, Wang G, Chen D, Lv X, Li J (2008) Tuning photoelectrochemical performances of Ag-$TiO_2$ nanocomposites via reduction/oxidation of Ag. Chem Mater 20:6543–6549
24. Liu YP, Fang L, Lu HD, Li YW, Hu CZ, Yu HG (2012) One-pot pyridine-assisted synthesis of visible-light-driven photocatalyst $Ag/Ag_3PO_4$. Appl Catal B Environ 115-116:245–252
25. Jiang J, Zhao K, Xiao XY, Zhang LZ (2014) Synthesis and facet-dependent photoreactivity of BiOCl single-crystalline nanosheets. J Am Chem Soc 134: 4473–4476
26. Izumi H, Nishihara Y (2000) Electronic structure of $BiPbO_2Cl$ as a two-dimensional analogue of $BaPb_xBi_{1-x}O_3$. J Phys Rev B 61:9855–9858
27. Yu J, Dai G, Huang B (2009) Fabrication and characterization of visible-light-driven plasmonic photocatalyst Ag/AgCl/$TiO_2$ nanotube arrays. J Phys Chem C 113:16394–16401